Investigation of the sensitivity of GOSAT TIR observations to CH_4 in the near-surface layer

Dmitry A. Belikov[1], Naoko Saitoh[1], Prabir K. Patra[2,1],

[1]*Center for Environmental Remote Sensing (CEReS), Chiba University, Chiba, Japan*

[2]*Research Institute for Global Change (RIGC), JAMSTEC, Yokohama, Japan*

Email: d.belikov@chiba-u.jp

CHIBA UNIVERSITY

Introduction

- We investigated the sensitivity of the thermal infrared (TIR) band observations of CH4 (TIR CH_4) by the Thermal And Near-infrared Sensor for carbon Observation-Fourier Transform Spectrometer (TANSO-FTS) onboard the Greenhouse gases Observation SATellite (GOSAT) in the lower part of the troposphere at the level of 950-850 hPa.
- GOSAT-TIR CH_4 was intercompared with CH_4 from the World Data Centre for Greenhouse Gases (WDCGG) ground observations and the MIROC4.0-based Atmospheric Chemistry Tracer Model (MIROC4-ACTM) model for the period 2009-2014.
- Comparison with the monthly, daily, and hourly measurements showed that GOSAT-TIR observations have a sufficiently high density of observations to detect the variability of CH_4 with different time scales.
- Good agreement with the WDCGG observations increases the reliability and confidence of the global distribution of GOSAT-TIR CH_4 and the possibility of its application for the validation of three-dimensional methane products.
- The date availability extension for the period 2014-2020 and beyond is essential for a more detailed analysis of the global three-dimensional distribution of methane.

GOSAT thermal infrared (TIR) band

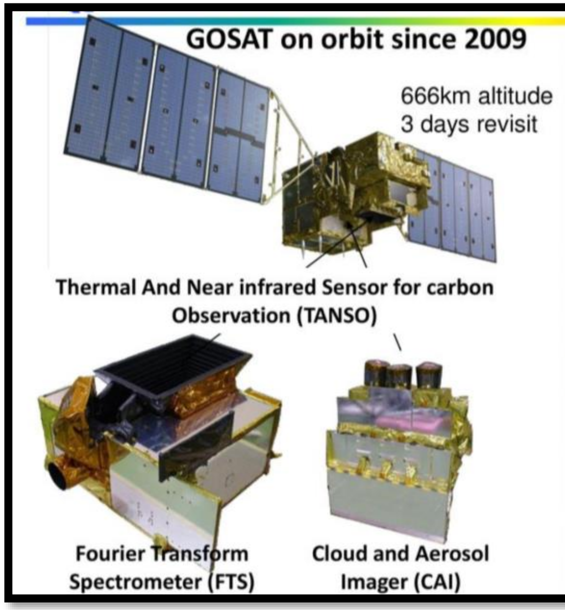

Fourier Transform Spectrometer (FTS)	
Mission	GHGs measurements
Band	SWIR-0.76μm, 1.6μm, 2.0μm bands with P/S polarization (O_2-A, CO_2, CH_4, H_2O band)
	TIR-5.5~14.3μm (CO_2, CH_4, O_3 band)
SPC Res.	$0.2cm^{-1}$
Swath	750km(3 points every 260km)
IFOV	10.5km

Cloud and Aerosol Imager (CAI)	
Mission	Cloud detection and aerosol correction within FTS IFOV
Band	Nadir view 0.38, 0.67, 0.87, 1.60μm band
Swath	750-1000km
Footprint	0.5 and 1.5km

by Kei Shiomi, JAXA

GOSAT-TIR benefits

1. Observations could be performed at night and during heavy cloud conditions
2. Captures signal at 22 layers from the top of the atmospheric boundary layer (ABL) up to UT/LS (800-150 hPa)
3. The sensitivity maximum at the levels of 200–400 hPa

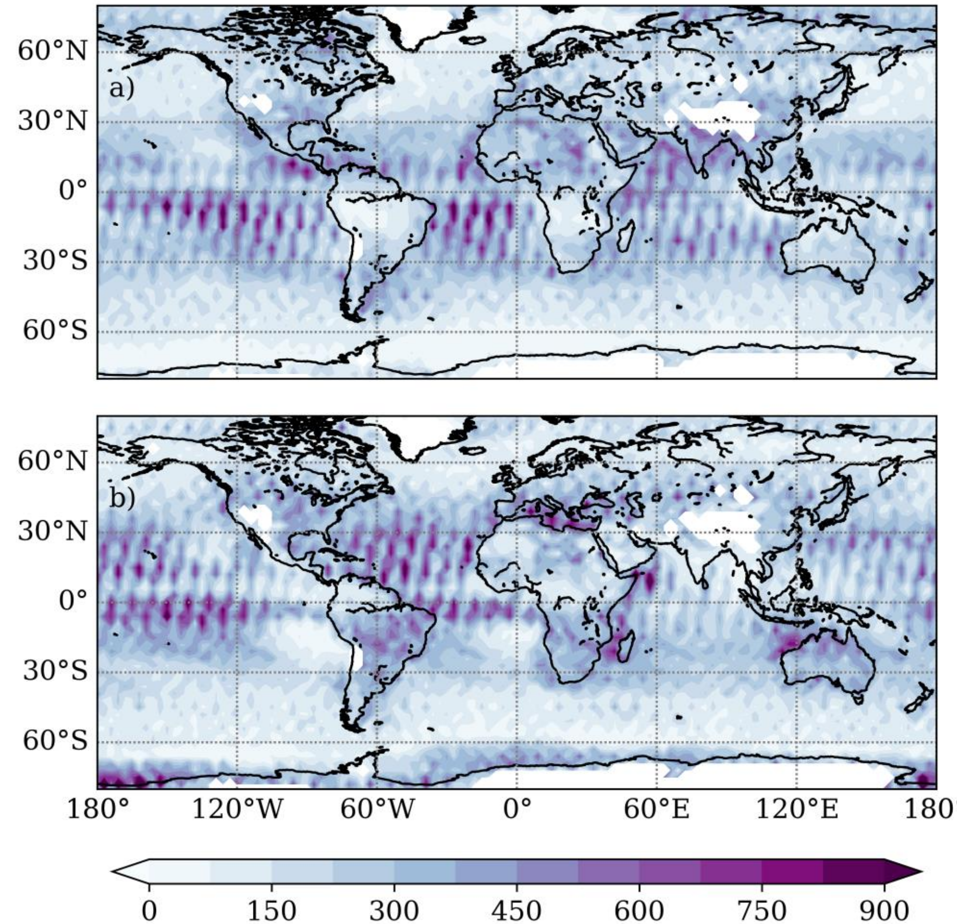

Figure 1. The mean number of observations per year from the GOSAT-TIR instrument at the levels of 850 - 950 hPa for the period 2010-2013, for JFM (a) and JAS (b) respectively. The data are remapped to the regular 3° × 3° grid.

WDCGG dataset

- WDCGG has been operated by the Japan Meteorological Agency (JMA) since 1990
- WDCGG provides critical services to the community through data collection, archiving, and distribution of data on (such as CO_2, CH_4, CFCs, N_2O) and related gases (such as CO) in the atmosphere and oceans from surface stations, mobile platforms, and satellites worldwide.
- Considering the gaps in the observed time series, we filtered out only those sites where the share of omissions during the study period does not exceed 20%. As a result, in our analysis, we selected 72, 26, and 23 sites performing monthly, daily, and hourly observations, respectively

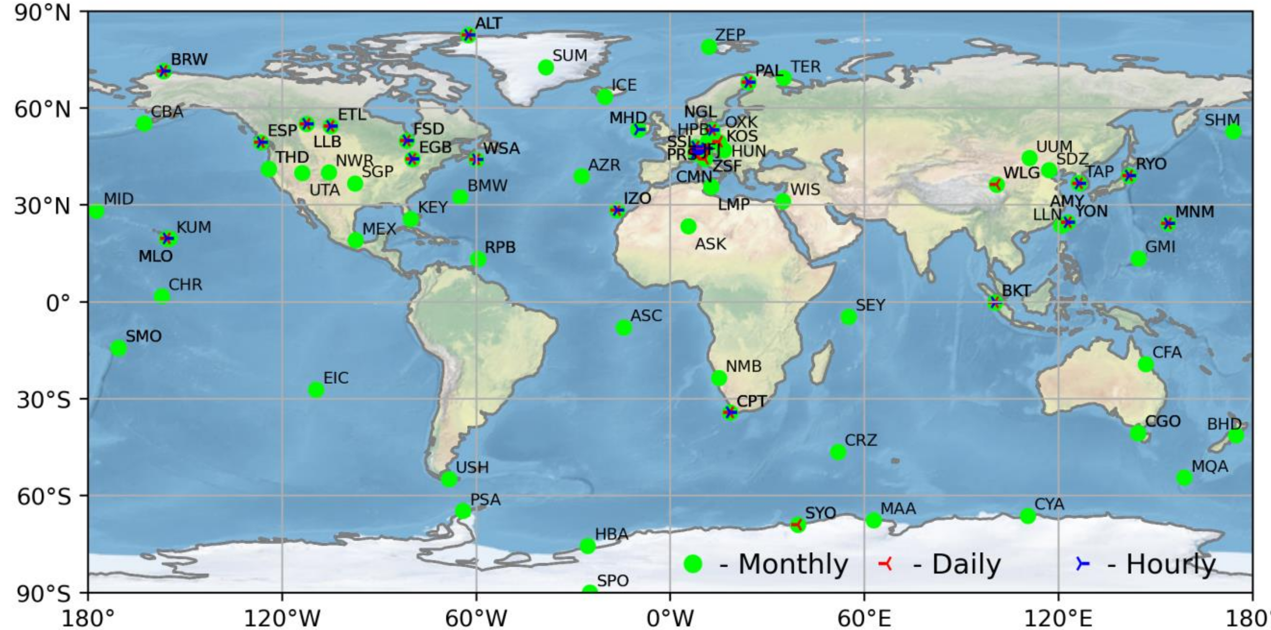

Figure 2. Location of the WDCGG observation sites. Here, green, red, and blue symbols show stations conducting measurements with monthly, daily, and hourly frequency. One station can simultaneously carry out measurements with different time periods (e.g., IZO, MNM).

The MIROC4.0-ACTM simulation setup

MIROC4-ACTM

CH_4 simulated by MIROC4-ACTM [Patra et al., 2018]:

- 67 sigma-pressure vertical layers (1000-0.01 hPa)
- horizontal grid T42 (lat/lon ~2.8 × 2.8°)
- U, V, T are nudged to JRA-55 reanalysis fields

Set of a priori fluxes

The a priori fluxes provided by the GCP protocol and associated to the oxidant fields from TRANSCOM

a) Cyclic: geological, ocean, termites, wetlands
b) IAV: biomass burning, biofuels, coal, livestock, oil + gas, rice, soils, waste

Chemical reactions

The chemical loss due to OH reactions is following [Patra et al., Nature, 2014].

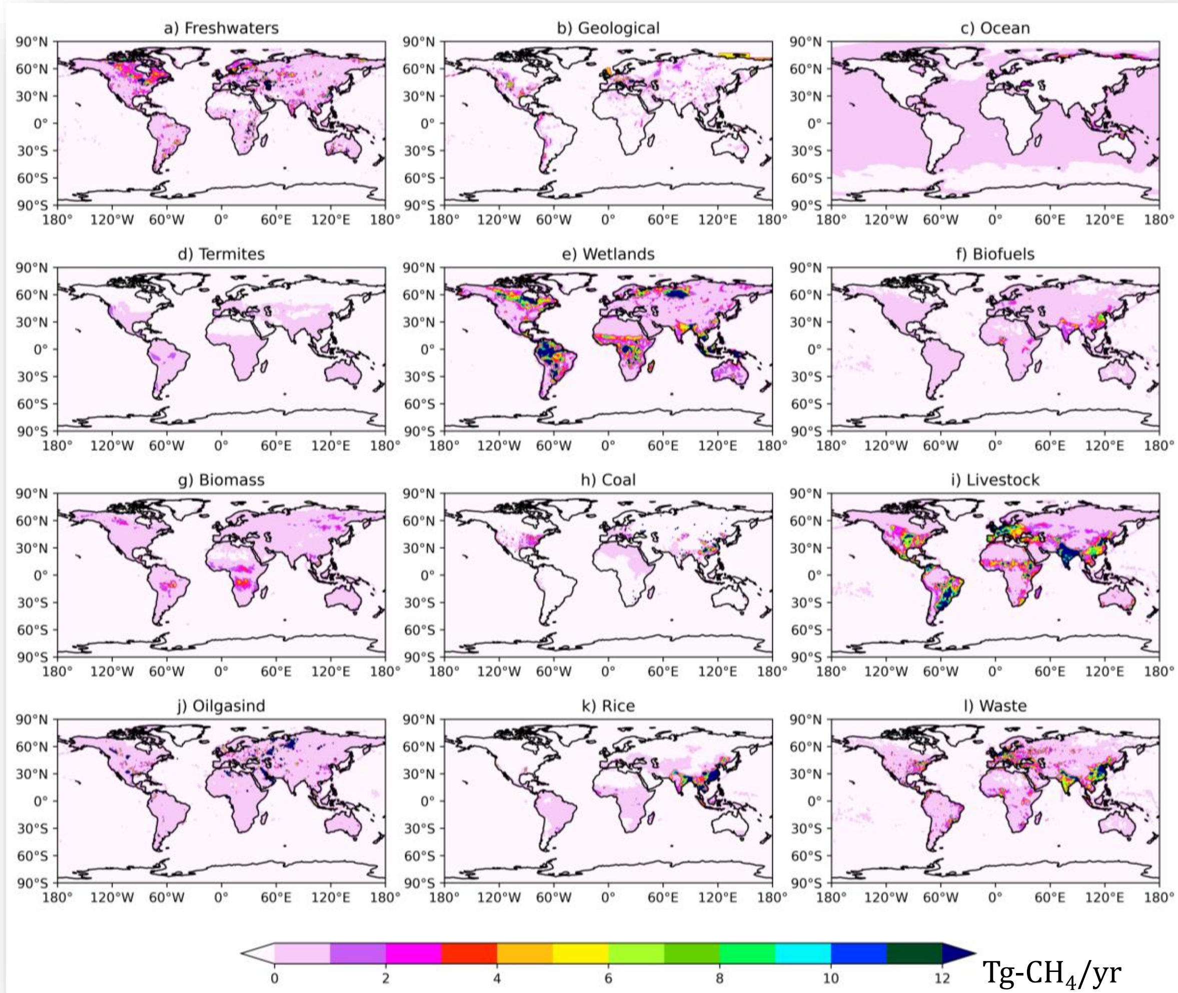

Figure 3. The a priori CH_4 fluxes.

Data comparison metrics

Unless additionally indicated the work aims to estimate GOSAT-TIR performance relative to GOSAT a priori (ACTM) by comparing corresponding time series derived for each site using the following metrics:

- Correlation coefficient r (hereafter, the Pearson correlation coefficient is used) between CH_4 from TIR (CH_4^{TIR}) and a priori (CH_4^{TIR}) in respect to observed CH_4 (CH_4^{obs}), defined as

$$r_x = \frac{\sum(x_i - \bar{x})(y_i - \bar{y})}{\sqrt{\sum(x_i - \bar{x})^2 \sum(y_i - \bar{y})^2}}$$

  where $x = \{CH_4^{TIR},\ CH_4^{prior},\ CH_4^{ACTM}\}, y = CH_4^{obs}$, $\bar{x}$ and $\bar{y}$ are the mean of the values of the x-variable and y-variable, respectively.

- Root mean square error (RMSE) between CH_4 from TIR and a priori in respect to observed CH_4, defined as

$$RMSE_x = \sqrt{\frac{\sum_{i=1}^{N}(y_i - x_i)^2}{N}}$$

  where $x = \{CH_4^{TIR},\ CH_4^{prior},\ CH_4^{ACTM}\}, y = CH_4^{obs}$, N is the number of non-missing data points.

- Standard deviation (SD) of the discrepancy between CH_4 from TIR and a priori in respect to the observed CH_4, defined as $CH_4^{TIR-obs} = CH_4^{TIR} - CH_4^{obs}$, $CH_4^{prior-obs} = CH_4^{prior} - CH_4^{obs}$, $CH_4^{ACTM-obs} = CH_4^{ACTM} - CH_4^{obs}$, respectively. The standard deviation equation is then:

$$\sigma_x = \sqrt{\frac{\sum_{i=1}^{N}(x_i - \bar{x})^2}{N}}$$

  where $x = \{CH_4^{TIR-obs},\ CH_4^{prior-obs},\ CH_4^{ACTM-obs}\}$, $\bar{x}$ is the x-variable mean, N is the number of non-missing data points.

Collocation with the WDCGG observations

- Here, we employed a straightforward collocation method that selects all observations within a 3-, 5-, 7, 10, or 15° radius of the monthly WDCGG stations, providing a substantial number of observations (Table 1).
- Even the smallest radius of 3° provides from 28 to 140 GOSAT-TIR samples/month, with average and median values of 85 and 83 samples/month, respectively.
- When the radius is 5, 7, 10, and 15°, the number of selected samples increase by about 3, 5, 10, and 23 times, respectively.

Number of the GOSAT-TIR observation points inside the collocation radius, points/month	Collocation radius size, °				
	3	5	7	10	15
Min	28	80	139	269	563
Max	140	410	753	1462	3040
Median	85	245	461	930	2130
Average	83	232	443	879	1936

Table 1. A monthly mean estimated dependence of the GOSAT-TIR observation point numbers used in the collocation on the size of the colocation radius.

Radius	Monthly observations			Daily observations			Hourly observations		
	Corr. Coef.	RMSE	SD	Corr. Coef.	RMSE	SD	Corr. Coef.	RMSE	SD
3	0.71	18.11	14.46	**0.52**	37.05	34.11	**0.52**	37.52	33.78
5	0.72	17.46	13.89	0.49	36.71	33.83	0.51	36.20	33.04
7	0.73	**17.05**	13.46	0.48	36.44	33.56	0.50	35.47	32.29
10	**0.74**	17.16	**13.25**	0.46	35.42	32.37	0.48	34.90	31.03
15	0.72	17.81	13.48	0.44	**34.18**	**31.04**	0.46	**34.79**	**30.27**

Table 2. Correlation coefficient, RMSE, and SD calculated for CH_4 from the GOSAT-TIR and WDCGG observations for different collocation radiuses and site sets.

Comparison with the monthly observations

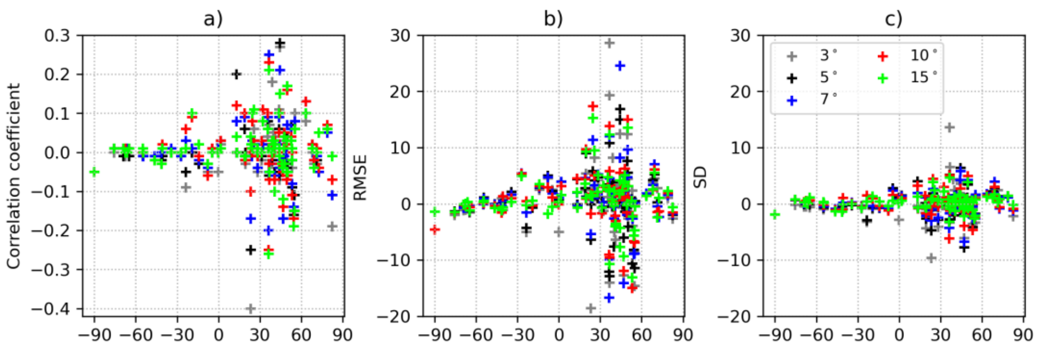

Figure 4. Latitude distributions of improvements compared to the monthly WDCGG observation derived for a) correlation coefficient, b) RMSE, c) 1-σ SD calculated from the CH_4 concentration from the GOSAT-TIR product and GOSAT a priori collocated using the different radius sizes for the considered period.

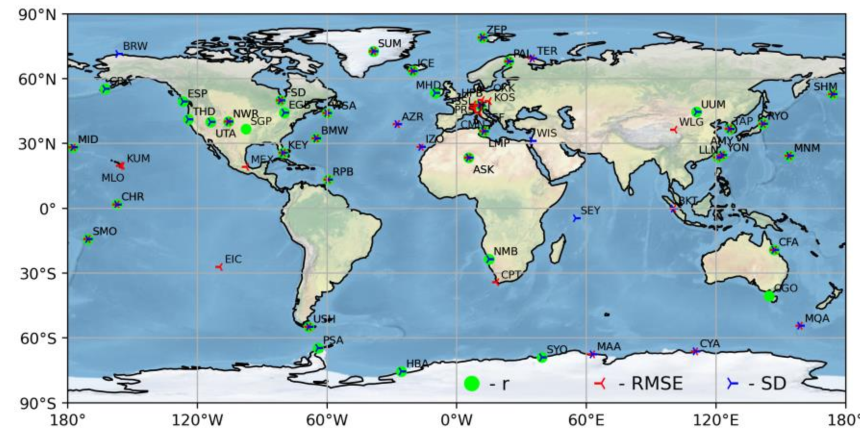

Figure 5. Symbols represent the WDCGG observation site locations where GOSAT-TIR CH_4 shows improved performance in comparison with the GOSAT a priori CH_4 using correlation coefficient (green), root mean square error (red), and the 1-σ SD (blue), respectively. The 15° collocation radius was used.

- The monthly WDCGG observations provide a comparison of a larger sample of stations located in a variety of climatic conditions.
- Gradual improvement from small to large radius. Thus, for a radius of 3°, the GOSAT-TIR CH_4 improved relative to the GOSAT a priori CH_4 at 18 from 72 sites according to all 3 metrics. If only one metric is considered the number of such sites is 46. For the case of 15° radius, the site numbers are increased to 24 and 61 respectively (Fig. 4).
- For all three metrics used, a general trend is noticeable, indicating the ability of the GOSAT-TIR to capture an additional signal over the coastal and remote sites located mainly in the northern hemisphere. A significant achievement was revealed in the middle and high latitudes. At the same time, the improvement for inland sites is minor mainly (Fig. 5).

Comparison with the daily observations

- Out of the 76 stations, 26 met the filtering criteria.
- At least one parameter is improved for all stations, regardless of the collocation method.
- For 5-7 stations, all three parameters were improved simultaneously. However, as Table 2 shows, it is impossible to simultaneously improve the correlation coefficient and the RMSE, as the first parameter worsens and the second one improves with an increased number of samples.

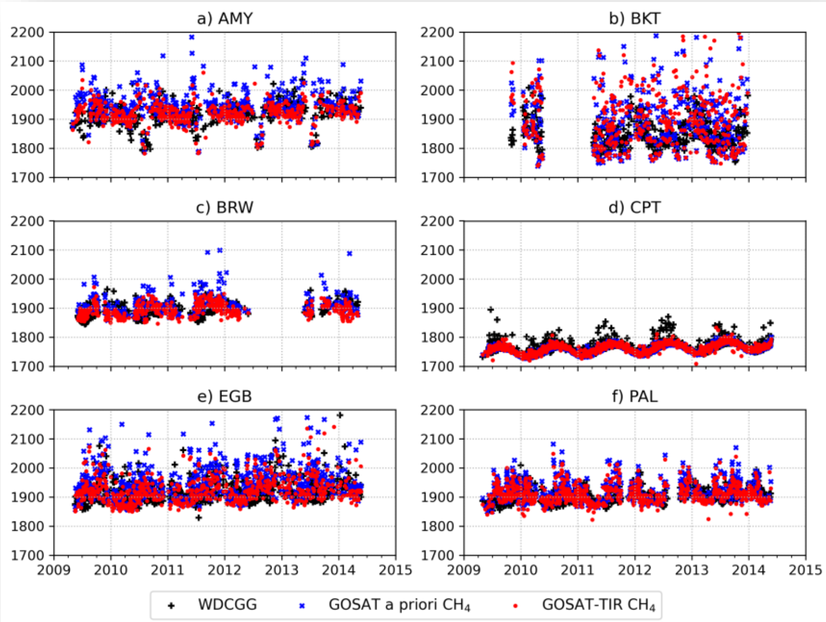

Figure 6. Seasonal variation of daily CH_4 derived from WDCGG ground observations, GOSAT-TIR, and GOSAT a priori over observational sites: AMY, Korea [36.54, 126.33, 42.0]; BKT, Indonesia [-0.20, 100.32, 864.0], BRW, USA [71.32, -156.61, 11.00]; CPT, South Africa [-34.35, 18.49, 230.0]; EGB, Canada [44.23, -79.78, 255.0]; and PAL, Finland [67.97, 24.12, 560.0] obtained with the 3° collocation radius.

- The considered stations are in regions with varying climatic, meteorological, and emission conditions causing a significantly different effect of the correction in GOSAT-TIR CH_4.
- Although the general trend indicates a decrease in the number and amplitude of outliers (AMY, BRW), we also note a more evident prescription of the seasonal cycle in AMY in summer, summer spikes in the concentration of CPT, and just small adjustments in all parameters (BKT, BRW, PAL).
- The narrow radius provided a relatively small set of the GOSAT-TIR samplings that better described the shape of small fluctuations
- The wide radius covered more samples that reproduced the average climatic values without describing interannual fluctuations.

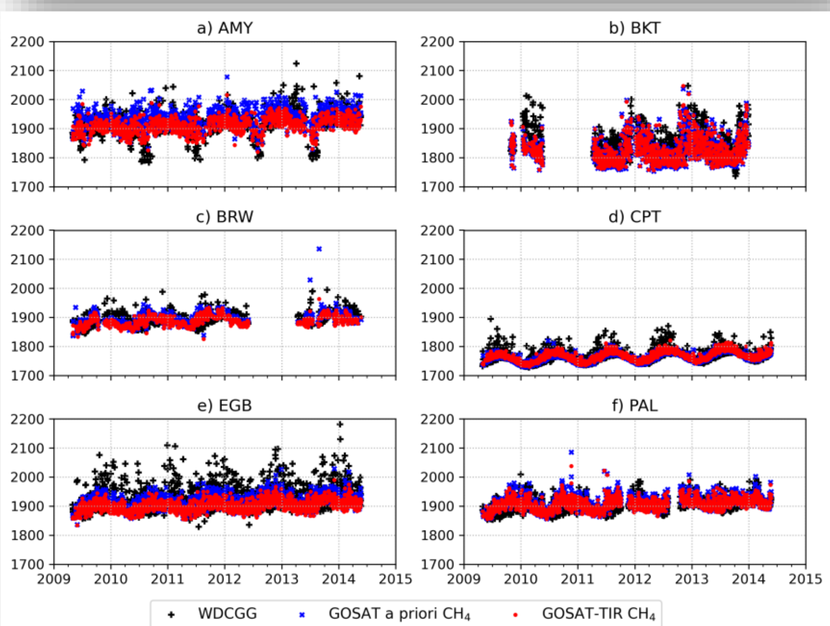

Figure 7. Same as Figure 6, but for the 15° collocation radius.

Comparison with the hourly observations

- The GOSAT makes two passes a day over a site. How well does GOSAT-TIR detect the diurnal variations of CH_4?
- In addition, two CH4 simulations based on the ACTM model were included in the comparison:
  - ACTM CH4: the model data were collocated with the time and coordinates of the satellite observations.
  - ACTMi CH4: the model data were only interpolated in space and kept a high temporal resolution of 1 hour.

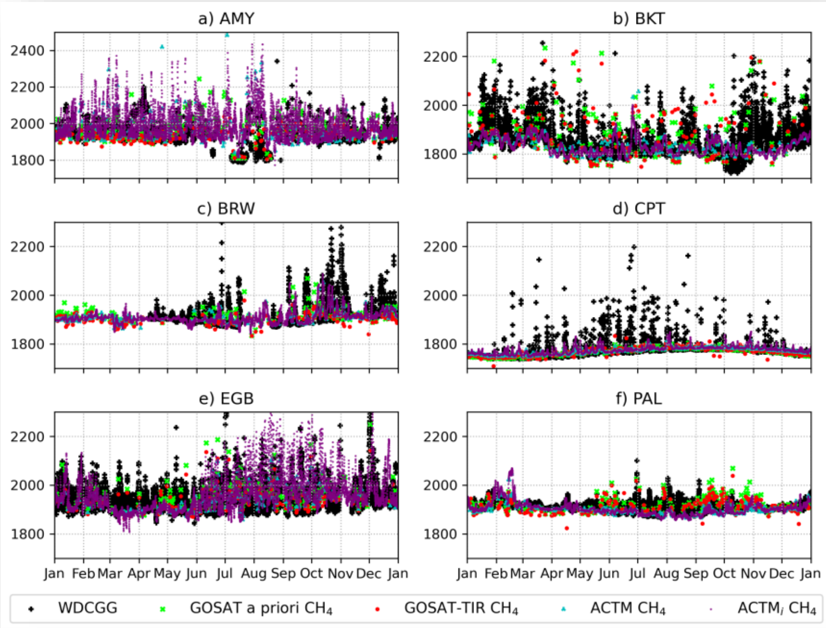

Figure 8. Seasonal variation of hourly CH_4 derived from WDCGG ground observations, GOSAT-TIR, GOSAT a priori, ACTM and ACTMi over observational sites: a) AMY, b) BKT, c) BRW, d) CPT, e) EGB, and f) PAL obtained with the 3° collocation radius for 2013.

- For BKT and BRW sites, all three datasets hardly reproduce the high-frequency oscillations, mainly due to the discrepancy in the occurrence of peak concentrations.
- For CPT and PAL, both model versions outperform GOSAT-TIR.
- For stations with the highest variability of CH_4 concentration during the year (AMY, EGB), GOSAT-TIR gives the best results. Apparently, due to its low sensitivity near the ground, this instrument captures only significant concentration peaks.
- The found superiority over the model with optimised fluxes emphasises the high uncertainty of the emissions at these sites.
- The simple collocation method can significantly bias the results in complex terrains such as BKT.

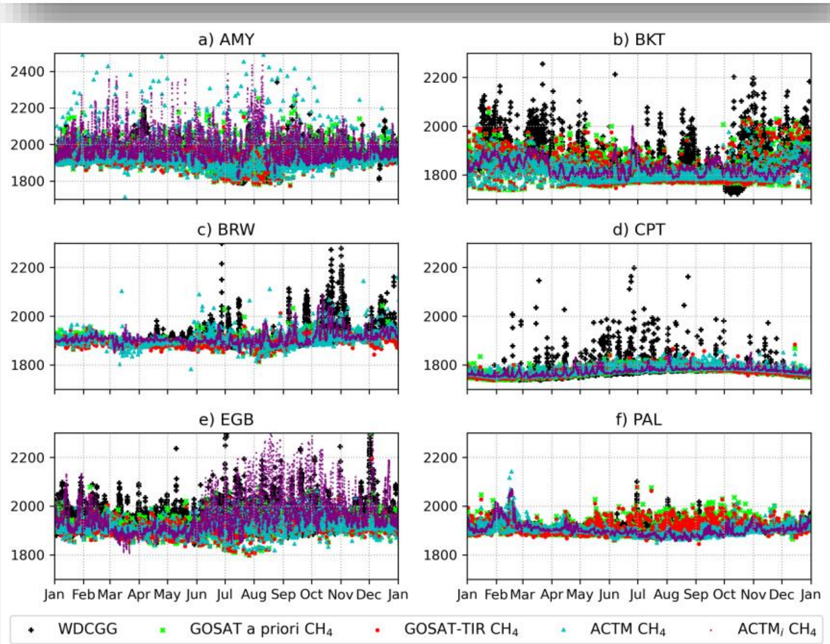

Figure 9. Same as Figure 8, but for the 15° collocation radius.

Summary

1. We investigated the sensitivity of the GOSAT-TIR CH_4 observations in the lower troposphere at the level of 950-850 hPA. For this purpose, GOSAT-TIR CH_4 was compared with CH_4 from WDCGG ground observations and the ACTM model for the period 2009-2014.
2. The comparison with monthly, daily and hourly measurements showed that the GOSAT-TIR observations have a sufficiently high observation density to detect the variability of CH_4 on different time scales.
3. We analysed the effect of the simple collocation method, which selects all observations within a radius of 3, 5, 7, 10 or 15°, reflecting the characteristics of the WDCGG observation footprint.
4. For the monthly datasets, the footprint is much larger, so the correlation improves with increasing radius, reaching a maximum at 10°.
5. The short-term observations (daily, hourly) have a much smaller footprint, so including a larger number of points outside this footprint by increasing the radius worsens the correction. The optimal values for RMSE and SD are achieved on a sample of several hundred of the GOSAT samples.
6. Overall, there is no one-size-fits-all collocation method for a large and diverse set of stations. Depending on the location, the preferred metric and the concentration gradient, it is possible to choose the best option. However, this task may require significant time and computational resources.
7. A good agreement with the WDCGG observations increases the reliability and confidence of the global distribution of GOSAT TIR CH_4 and the possibility to use it for the validation of three-dimensional methane products.
8. The extension of data availability for the period 2014-2020 and beyond is essential for a more detailed analysis.